ANALYTICAL SOLUTIONS FOR PARTICLE TRACKING IN PLANAR CRYSTAL CHANNELLING

A. Iliopoulou*[1,2], B. Lindström[1,3], S. Van der Schueren[1,4], F. F. Van der Veken[1], D. Veres[1,5]
[1]CERN, Meyrin, Switzerland, [2]University of Macedonia, Thessaloniki, Greece
[3]John Adams Institute at Royal Holloway, University of London, Egham, UK
[4]Sapienza University, Rome, Italy, [5]Goethe University, Frankfurt am Main, Germany

Abstract

Planar particle channelling describes the motion of high-energy particles trapped in the potential well formed by crystal lattice planes, allowing their trajectories to be deflected in a controlled manner. Within the Molière approximation, which incorporates atomic screening and thermal vibrations, this motion is typically either approximated by a harmonic potential or evaluated numerically. Here, we propose a simplified Molière model that yields closed-form analytical solutions expressed through Jacobi elliptic functions. To extend the treatment to bent crystals, symplectic integrators are applied to the equations of motion, ensuring accuracy and long-term stability through symplecticity. This semi-analytical approach to evaluate bent channelling has been benchmarked against existing numerical methods, and the optimal configuration will be integrated into Xsuite's Xcoll package.

INTRODUCTION

Crystals are used in the CERN accelerator complex for a series of applications, including beam extraction [1–3], crystal collimation [4–7], and exotic particle measurements [8–14]. Their significant advantages include a strong beam-bending capability while requiring no additional space due to their small size[1]. Compared to magnets, which inevitably affect the entire beam, crystals influence only the intercepted particles, leaving the rest of the beam untouched [15].

The implementation of crystals into simulations requires studying the underlying particle–matter interactions, such as channelling, dechannelling, volume capture, and volume reflection [16]. Here we focus on the channelling process.

Thus far, existing simulation tools employ either the harmonic approximation of the potential [16, 17], which lacks sufficient accuracy, or a stepwise numerical solution to the Molière model [18], which is computationally expensive.

This paper introduces a new model, based on a simplified Molière potential, which aims to combine adequate accuracy with computational efficiency and is intended for implementation in Xcoll [19, 20], the collimation module of the Xsuite simulation library [21, 22].

MODEL DESCRIPTION

Our model is derived from the Molière potential for a "warm" atomic plane [16], approximating the sum of exponentials by a single exponential, leading to the relation below:

$$U(x) = U_{\mathrm{N}} \left(\cosh \frac{\beta_{\mathrm{i}}}{a_{\mathrm{TF}}} x - 1 \right), \tag{1}$$

$$U_{\mathrm{N}} = 2U_{\max} \frac{\alpha_{\mathrm{i}}}{\beta_{\mathrm{i}}} \, \mathrm{e}^{-\frac{\beta_{\mathrm{i}}}{a_{\mathrm{TF}}} \frac{d_{\mathrm{P}}}{2}}, \tag{2}$$

where[2] $a_{\mathrm{TF}} = 0.4683\, Z^{-1/3}$Å is the so-called screening distance, d_{P} is the planar spacing, and $U_{\max} = 2\pi N Z_{\mathrm{i}} Z e^2 d_{\mathrm{P}}\, a_{\mathrm{TF}}$. For the ^{28}Si (110) plane, we have $U_{\max} = 23.9037$ eV, $d_{\mathrm{P}} = 1.92$ Å, and $a_{\mathrm{TF}} = 0.194$ Å. The parameters $\alpha_{\mathrm{i}} = 0.722452$ and $\beta_{\mathrm{i}} = 0.573481$ are determined empirically to reproduce the original Molière potential with an observed accuracy up to 0.068 eV over the interval $[-x_{\mathrm{c}}, x_{\mathrm{c}}]$, where x_{c} is the maximum amplitude allowed for the particle oscillation.[3]

CHANNELLING EQUATION

Under the continuum approximation, assuming a classical particle trajectory with small angles relative to the crystal lattice planes ($\theta \approx \tan\theta = \frac{p_x}{p_z}$), adiabatic invariance (no energy losses), and a thermally averaged crystal, the particle transverse energy is considered a constant of motion:

$$E_{\mathrm{T}} = \frac{1}{2}\beta p c \theta^2 + U(x) = \text{constant}.$$

The channelling equation is then reduced to a one-dimensional differential equation [23]:

$$\beta p c x''(s) + \partial_x U(x) = 0, \tag{3}$$

where s is the direction of motion along the (potentially curved) path and x is the transverse coordinate along which the oscillation occurs.

Straight Crystal

For a straight crystal, one can substitute Eq. (1) into Eq. (3), leading to analytical solutions expressed in terms of Jacobi elliptic functions [24] as follows:

$$x(z) = 2\mathrm{i} \frac{a_{\mathrm{TF}}}{\beta_{\mathrm{i}}} \, \mathrm{am}\left(\mathrm{i}(\nu z + \phi) \, , \, -2\frac{U_{\mathrm{N}}}{E_{\mathrm{T}}} \right),$$

$$\theta(z) = -2 \frac{a_{\mathrm{TF}}}{\beta_{\mathrm{i}}} \nu \, \mathrm{dn}\left(\mathrm{i}(\nu z + \phi) \, , \, -2\frac{U_{\mathrm{N}}}{E_{\mathrm{T}}} \right),$$

* anastasia.iliopoulou@cern.ch

[1] Typically on the mm–cm scale.

[2] N denotes the atomic density of the crystal, Z the atomic number of the lattice atoms, Z_{i} the charge number of the incident particle and e the elementary charge, as explained in Ref. [16].

[3] Based on measurements, we typically use $x_{\mathrm{c}} = \sqrt{0.9}\, \frac{d_{\mathrm{P}}}{2}$ but this can be optimised.

with

$$\nu = -\mathrm{sgn}(\theta_{\mathrm{in}})\frac{\beta_{\mathrm{i}}}{a_{\mathrm{TF}}}\sqrt{\frac{E_{\mathrm{T}}}{2\beta pc}},$$
$$\phi = -\mathrm{i}\ \mathrm{F}\left(-\frac{\mathrm{i}}{2}x_{\mathrm{in}}\frac{\beta_{\mathrm{i}}}{a_{\mathrm{TF}}}\ ,\ -2\frac{U_{\mathrm{N}}}{E_{\mathrm{T}}}\right),$$

where $\mathrm{am}(u,m)$ is the Jacobi amplitude, $\mathrm{dn}(u,m)$ is the Jacobi delta amplitude, $\mathrm{F}(\phi,m)$ is the incomplete elliptic integral of the first kind, and $(x_{\mathrm{in}},\theta_{\mathrm{in}})$ are the initial conditions of the particle entering the crystal.

Although the Jacobi elliptic functions are defined for $u,\phi\in\mathbb{R}$ and $0\le m\le 1$, their domain can be extended by means of analytical continuation [25].

To implement these solutions in a computational environment, it is necessary to transform them into the standard function domain. This can be achieved by applying mathematical identities [24], which result in:

$$x(z) = -2\frac{a_{\mathrm{TF}}}{\beta_{\mathrm{i}}}\sinh^{-1}\left(\sqrt{m'}\frac{\mathrm{sn}\left(\sqrt{m}\,(\nu z+\phi),m'\right)}{\mathrm{dn}\left(\sqrt{m}\,(\nu z+\phi),m'\right)}\right),$$
$$\theta(z) = -2\frac{a_{\mathrm{TF}}}{\beta_{\mathrm{i}}}\nu\frac{\mathrm{cn}\left(\sqrt{m}\,(\nu z+\phi),m'\right)}{\mathrm{dn}\left(\sqrt{m}\,(\nu z+\phi),m'\right)},$$

where $m = 1+2\frac{U_{\mathrm{N}}}{E_{\mathrm{T}}}$, $m' = \frac{1}{m}$, and

$$\phi = \sqrt{m'}\ \mathrm{F}\left(\frac{mU(x_{\mathrm{in}})}{U(x_{\mathrm{in}})+2U_{\mathrm{N}}},m'\right),$$

while $\mathrm{sn}(u,m)$ and $\mathrm{cn}(u,m)$ are the Jacobi elliptic sine and cosine functions, respectively, and ν remains unchanged after the transformation.

Bent Crystal

For the aforementioned applications in the CERN accelerator complex, the crystals employed are bent, meaning that the motion can be described by an effective potential, including the bending term:

$$U_{\mathrm{eff}}(x) = U(x)+\frac{\beta pc}{R}x,$$

where R is the bending radius and is considered constant throughout this work.

In this case, purely analytical solutions to the simplified Molière potential no longer exist. In this work, we therefore use a symplectic integration scheme, which splits the Hamiltonian into two parts, H_1 and H_2, each of which can be solved exactly, and composes their flows in a way that preserves the symplectic structure. Our study benchmarks three different Hamiltonian splitting approaches.

The Hamiltonian can be written as:

$$H = \frac{\beta pc}{2}\theta^2+U_{\mathrm{N}}\left[\cosh\left(\frac{\beta_{\mathrm{i}}}{a_{\mathrm{TF}}}x\right)-1\right]+\frac{\beta pc}{R}x,$$

and the splitting methods executed are[4]:

[4] Method 1 was an alternative way to split the Hamiltonian, but was shown not to be convergent and hence abandoned; the naming is retained for consistency with prior communication.

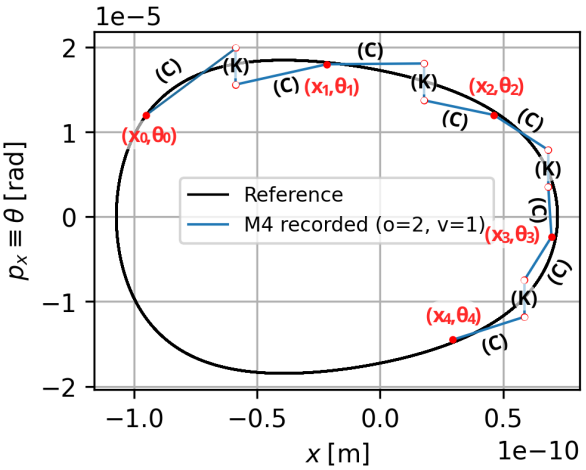

Figure 1: The first four points in symplectic integration, illustrating the channel (C) – kick (K) - channel (C) sequence.

Method 2 (M2):

$$H_0 = \frac{\beta pc}{2}\theta^2+\frac{U_{\mathrm{N}}}{2}\left(\frac{\beta_{\mathrm{i}}}{a_{\mathrm{TF}}}x\right)^2,$$
$$H_{\mathrm{IB}} = U_{\mathrm{N}}\left[\cosh\left(\frac{\beta_{\mathrm{i}}}{a_{\mathrm{TF}}}x\right)-1-\frac{1}{2}\left(\frac{\beta_{\mathrm{i}}}{a_{\mathrm{TF}}}x\right)^2\right]+\frac{\beta pc}{R}x,$$

Method 3 (M3):

$$H_{\mathrm{B0}} = \frac{\beta pc}{2}\theta^2+\frac{U_{\mathrm{N}}}{2}\left(\frac{\beta_{\mathrm{i}}}{a_{\mathrm{TF}}}x\right)^2+\frac{\beta pc}{R}x,$$
$$H_{\mathrm{I}} = U_{\mathrm{N}}\left[\cosh\left(\frac{\beta_{\mathrm{i}}}{a_{\mathrm{TF}}}x\right)-1-\frac{1}{2}\left(\frac{\beta_{\mathrm{i}}}{a_{\mathrm{TF}}}x\right)^2\right],$$

Method 4 (M4):

$$H_{\mathrm{exact}} = \frac{\beta pc}{2}\theta^2+U_{\mathrm{N}}\left[\cosh\left(\frac{\beta_{\mathrm{i}}}{a_{\mathrm{TF}}}x\right)-1\right],$$
$$H_{\mathrm{B}} = \frac{\beta pc}{R}x.$$

The first part of the Hamiltonian can be identified as a generalised channelling (C) and the second part as a generalised kick (K). The two sequences that can be selected to construct a full integration step (Fig. 1) are:

Version 1 (V1): $x_0 \underset{\text{channel}}{\longrightarrow} x_1 \underset{\text{kick}}{\longrightarrow} x_2 \underset{\text{channel}}{\longrightarrow} x_3,$

Version 2 (V2): $x_0 \underset{\text{kick}}{\longrightarrow} x_1 \underset{\text{channel}}{\longrightarrow} x_2 \underset{\text{kick}}{\longrightarrow} x_3.$

We can further divide the steps into symmetric sub-steps to improve precision through different integration orders (O) as defined by the Yoshida approach [26], which indicate the number of sub-steps per step.

BENCHMARKING RESULTS

After applying the three approaches, M2, M3, and M4, to a set of 13 different initial conditions and all combinations of orders and versions, the results were benchmarked

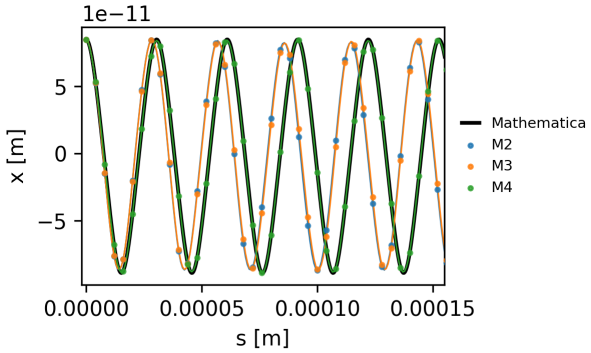

Figure 2: Comparison to the Mathematica solution for a given order/version (O2/V1) and integration steps.

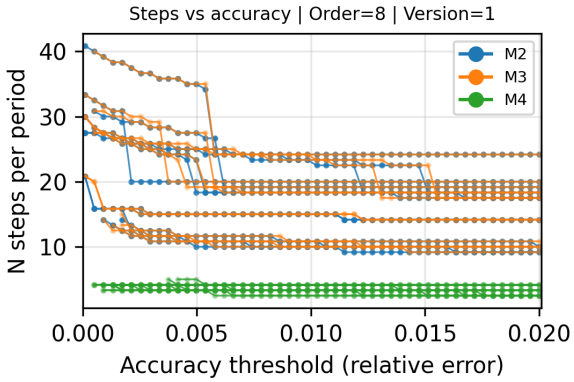

Figure 3: Number of points per period (N) to attain a specific accuracy thresholds for O8/V1.

against high-precision numerical solutions obtained with Mathematica [27]. The general case tested corresponded to a ^{28}Si (110) crystal plane with length $L = 0.4$ mm, and we scanned all combinations of methods, orders, and versions for 10 to 600 integration steps over the full crystal length. As shown in Fig. 2, M4 exhibits remarkably good convergence compared to M2 and M3.

From the full scan, we collected the successful runs, defined as those that achieve a relative error of less than 2%. By comparing the minimum number of steps (N) per period required to reach a given accuracy threshold, we concluded that M4 converges while requiring significantly fewer steps. As an example, Fig. 3 illustrates the N–accuracy plot for all models for O8/V1, representing the general trend observed for every O/V configuration.

Regarding versions and orders, the results show that O4 improves accuracy while having a similar runtime to O2 (Fig. 4), whereas higher orders are more computationally expensive than justified by their gain in precision (Fig. 5). Concerning the versions, V1 is observed to be more stable and accurate.

CONCLUSION AND OUTLOOK

A new method for modelling crystal channelling has been developed that is computationally faster than the conventional stepwise Molière tracking approach and significantly more accurate than the harmonic approximation.

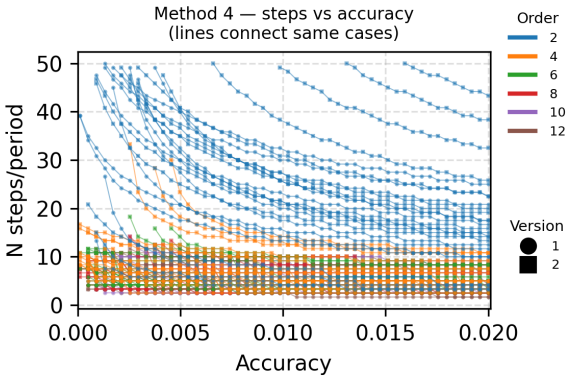

Figure 4: The smallest number of points (N) per period required for specific accuracy thresholds for all different integration orders in M4.

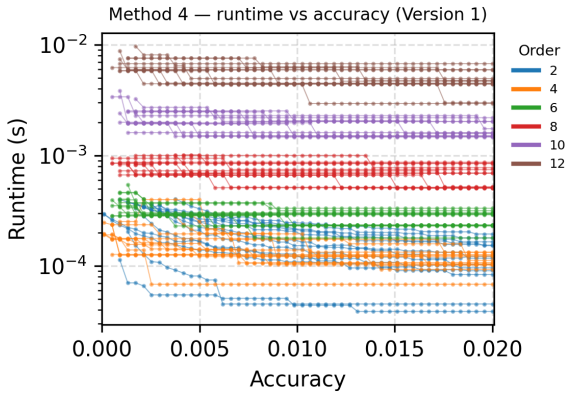

Figure 5: Runtimes for specific accuracy thresholds for all different integration orders in M4.

Different configurations were compared, finding that method 4, which implements a fourth order Yoshida integrator as straight channelling - bending kick - straight channelling, is the most computationally stable and reliable approach, providing the optimal balance between runtime and accuracy.

As a next step, we plan to fully integrate this model into the Xsuite/Xcoll framework, with O4/V1 as the default configuration, taking into account the physical limitations of channelling conditions.

Further benchmarking against experimental data is required to assess the accuracy of the approach, and additional crystal–particle interaction mechanisms, such as volume reflection, will be incorporated.

ACKNOWLEDGEMENTS

The authors would like to thank Dr. Giovanni Iadarola and Dr. Riccardo De Maria for their contributions to previous related work and for helpful discussions.

REFERENCES

[1] D. E. Veres, M. Giovannozzi, and G. Franchetti, "Exploring the potential of resonance islands and bent crystals for a slow extraction from circular hadron accelerators", *Phys. Rev. Res.*, vol. 6, no. 4, p. L042018, Oct. 2024. doi:10.1103/PhysRevResearch.6.L042018

[2] D. E. Veres, M. Giovannozzi, and G. Franchetti, "An innovative method for slow extraction in circular hadron accelerators with resonance islands and bent crystals", *Nucl. Instrum. Methods Phys. Res., Sect. A*, vol. 1073, p. 170286, 2025. doi:10.1016/j.nima.2025.170286

[3] F. M. Velotti *et al.*, "Septum shadowing by means of a bent crystal to reduce slow extraction beam loss", *Phys. Rev. Accel. Beams*, vol. 22, no. 9, p. 093502, Sep. 2019. doi:10.1103/PhysRevAccelBeams.22.093502

[4] S. Redaelli *et al.*, "Crystal collimation of heavy-ion beams at the large hadron collider", *Phys. Rev. Accel. Beams*, vol. 28, no. 5, p. 051001, May 2025. doi:10.1103/PhysRevAccelBeams.28.051001

[5] W. Scandale, "Crystal-based collimation in modern colliders", *Int. J. Mod. Phys. A*, vol. 25, no. supp01, pp. 70–85, 2010. doi:10.1142/S0217751X1004992X

[6] R. P. Fliller *et al.*, "Results of bent crystal channeling and collimation at the relativistic heavy ion collider", *Phys. Rev. ST Accel. Beams*, vol. 9, no. 1, p. 013501, Jan. 2006. doi:10.1103/PhysRevSTAB.9.013501

[7] M. D'Andrea *et al.*, "Operational performance of crystal collimation with 6.37 *Z* TeV Pb ion beams at the LHC", *Phys. Rev. Accel. Beams*, vol. 27, no. 1, p. 011002, Jan. 2024. doi:10.1103/PhysRevAccelBeams.27.011002

[8] L. Bandiera *et al.*, "Performance of short and long bent crystals for the TWOCRYST experiment at the large hadron collider", *Eur. Phys. J. C*, vol. 85, p. 1373, Dec. 2025. doi:10.1140/epjc/s10052-025-15092-y

[9] E. Bagli *et al.*, "Electromagnetic dipole moments of charged baryons with bent crystals at the LHC", *Eur. Phys. J. C*, vol. 77, no. 12, p. 828, Dec. 2017. doi:10.1140/epjc/s10052-017-5400-x

[10] J. Fu *et al.*, "Novel Method for the Direct Measurement of the τ Lepton Dipole Moments", *Phys. Rev. Lett.*, vol. 123, no. 1, p. 011801, Jul. 2019. doi:10.1103/PhysRevLett.123.011801

[11] A. S. Fomin, A. Y. Korchin, A. Stocchi, S. Barsuk, and P. Robbe, "Feasibility of τ-lepton electromagnetic dipole moments measurement using bent crystal at the LHC", *J. High Energy Phys.*, vol. 2019, no. 3, p. 156, Mar. 2019. doi:10.1007/JHEP03(2019)156

[12] D. Mirarchi, A. S. Fomin, S. Redaelli, and W. Scandale, "Layouts for fixed-target experiments and dipole moment measurements of short-lived baryons using bent crystals at the LHC", *Eur. Phys. J. C*, vol. 80, no. 10, p. 929, Oct. 2020. doi:10.1140/epjc/s10052-020-08466-x

[13] S. Redaelli, M. Ferro-Luzzi, and C. Hadjidakis, "Studies for future fixed-target experiments at the LHC in the framework of the CERN physics beyond colliders study", in *Proc. IPAC'18*, Vancouver, Canada, Apr.-May 2018, pp. 798–801, 2018. doi:10.18429/JACoW-IPAC2018-TUPAF045

[14] J. Jaeckel, M. Lamont, and C. Vallée, "The quest for new physics with the physics beyond colliders programme", *Nat. Phys.*, vol. 16, no. 4, pp. 393–401, Apr. 2020. doi:10.1038/s41567-020-0838-4

[15] Søren. P. Møller, "High-energy channeling — applications in beam bending and extraction", *Nucl. Instrum. Methods Phys. Res., Sect. A*, vol. 361, no. 3, pp. 403–420, 1995. doi:10.1016/0168-9002(95)00181-6

[16] V. M. Biryukov, Y. A. Chesnokov, and V. I. Kotov, *Crystal channeling and its application at high-energy accelerators*. Berlin, Germany: Springer, 1997. doi:10.1007/978-3-662-03407-1

[17] D. Mirarchi, G. Hall, S. Redaelli, and W. Scandale, "A crystal routine for collimation studies in circular proton accelerators", *Nucl. Instrum. Methods Phys. Res., Sect. B*, vol. 355, pp. 378–382, 2015. doi:10.1016/j.nimb.2015.03.026

[18] E. Bagli, M. Asai, D. Brandt, A. Dotti, V. Guidi, and D. H. Wright, "A model for the interaction of high-energy particles in straight and bent crystals implemented in Geant4", *Eur. Phys. J. C*, vol. 74, no. 8, Aug. 2014. doi:10.1140/epjc/s10052-014-2996-y

[19] D. Demetriadou, A. Abramov, G. Iadarola, and F. F. Van der Veken, "Tools for integrated simulation of collimation processes in Xsuite", in *Proc. IPAC'23*, Venice, Italy, pp. 2801–2804, 2023. doi:10.18429/JACoW-IPAC2023-WEPA066

[20] F. F. Van der Veken *et al.*, "Recent developments with the new tools for collimation simulations in Xsuite", in *Proc. HB'23*, Geneva, Switzerland, pp. 474–478, Oct. 2024. doi:10.18429/JACoW-HB2023-THBP13

[21] G. Iadarola *et al.*, "Xsuite: an integrated beam physics simulation framework", in *Proc. HB'23*, Geneva, Switzerland, pp. 73–80, Oct. 2023. doi:10.18429/JACoW-HB2023-TUA2I1

[22] S. Łopaciuk, G. Iadarola, R. De Maria, and F. F. Van der Veken, "Empowering a broad and diverse community in beam dynamics simulations with Xsuite", in *Proc. IPAC'25*, Taipei, Taiwan, pp. 1702–1705, 2025. doi:10.18429/JACoW-IPAC2025-WEBN1

[23] J. Lindhard, "Influence of crystal lattice on motion of energetic charged particles", *Mat. Fys. Medd. Dan. Vid. Selsk.*, vol. 34, no. 14, 1965.

[24] M. Abramowitz and I. A. Stegun, *Handbook of mathematical functions, with formulas, graphs, and mathematical tables*, New York, NY, USA: Dover Publications, 1974.

[25] G. B. Arfken, H. J. Weber, and F. E. Harris, *Mathematical methods for physicists: a comprehensive guide*. Waltham, MA, USA: Academic Press, 2012. doi:10.1016/C2009-0-30629-7

[26] H. Yoshida, "Construction of higher order symplectic integrators", *Phys. Lett. A*, vol. 150, no. 5–7, pp. 262–268, 1990. doi:10.1016/0375-9601(90)90092-3

[27] Wolfram Research, Inc., Mathematica, Version 14.3, https://www.wolfram.com/mathematica